Fennoscandian Earthquakes: Whole Crustal Rupturing Related to Postglacial Rebound

Ronald Arvidsson*

Local and regional earthquake locations provide seismic evidence that large shield earthquakes have occurred in northern Fennoscandia. These paleoearthquakes, with fault lengths of up to 160 kilometers and average displacements of up to 15 meters, were triggered by nonisostatic compressive stresses caused by the removal of the ice at the end of the last deglaciation. The Fennoscandian faults were probably formed by single events that ruptured through most of the crust. The largest event, moment magnitude $M_W \approx 8.2$, was larger than other known stable continent earthquakes outside failed rifts or extended crust.

Large-scale surface lineaments (up to 160 km) in northern Fennoscandia (*1*) have been interpreted as postglacial fault scarps (PGFs) formed by thrust earthquakes shortly after the local deglaciation 9000 years ago. The formation of these faults may have been due to stresses caused by early postglacial rebound, and if so, the faults can be used to estimate the rate of early postglacial rebound and to infer lithospheric dynamics (*2*). Offsets of Quaternary sediments and the clustering of paleolandslides and liquefaction phenomena (*3*) along the scarps indicate that these faults mark Quaternary earthquakes. Such evidence would not be observable if the PGFs formed before deglaciation (*3*) and restricts the oldest age for the displacements on the PGFs to the time of local deglaciation, 8500 to 9000 years ago. The younger age limit is set by undisturbed postglacial sediments, including littoral sediments, that overlie parts of the Lansjärv PGF, glacier meltwater channels that cut through the Pärvie scarp, and ^{14}C dates of peat in a landslide close to Lansjärv of 8200 ± 200 years ago (*3*). The shallow littoral sediments have depths of <10 m and were formed within 200 years after deglaciation, after which, on the basis of the rate of landrise (*4*), they were raised above sea level. In view of the length of the faults in the stable shield of northern Fennoscandia, the causative earthquakes would have had magnitudes of ~8. Intraplate earthquakes of such magnitude have elsewhere only been located in failed rifts or extended crustal regions (*5*). I analyzed seismic data to determine whether the observed lineaments are due to earthquakes, and to estimate the likely magnitudes, fault dimensions, and number of events that produced the PGFs.

The existence of an active fault zone is typically indicated by a high concentration of seismicity. It has been shown for intraplate areas, like the studied region, that earthquake activity is observed around zones of crustal weakness (*6*). It has not been clear whether the present-day earthquakes in northern Fennoscandia occur in association with the PGFs (*3*, *7*). I investigated the spatial correlation between recent seismicity and PGFs using a catalog (*8*, *9*) of instrumental recordings from 1963 to 1993 (Fig. 1). Man-made explosions occurring in northern Sweden were excluded from the catalog by personnel at the Swedish Seismological Network. Due to the level of catalog completeness I only considered earthquakes with local magnitude, $M_L \geq 2.7$ (*10*). The analysis (*10*) revealed that about 50% of the earthquakes were associated with the PGFs, a much higher number than expected from random occurrence of seismicity (*10*). A correlation between earthquakes and the PGFs was also indicated by the more precise hypocenter locations of smaller microearthquakes, $M_L \leq 2.4$, near the Lansjärv fault (Fig. 2). The microearthquakes were recorded during two surveys performed by the Seismological Department, Uppsala University, in 1987 and 1988 (*11*). The microearthquake locations (*12*) were clustered along the length of the Lansjärv fault, and 84% of the hypocenters were in the block southeast of the scarp. The proximity of the microearthquakes to the scarp relates them to the Lansjärv PGF (90% of the events were located less than 15 km from the main fault). The diffuse distribution of hypocenters (Fig. 2) probably reflects complexity of the faulting; such a distribution is commonly observed for aftershock distributions of dip-slip earthquakes (*13*). The correlation of seismicity, including the microearthquakes, with the PGFs indicates that the scarps were formed

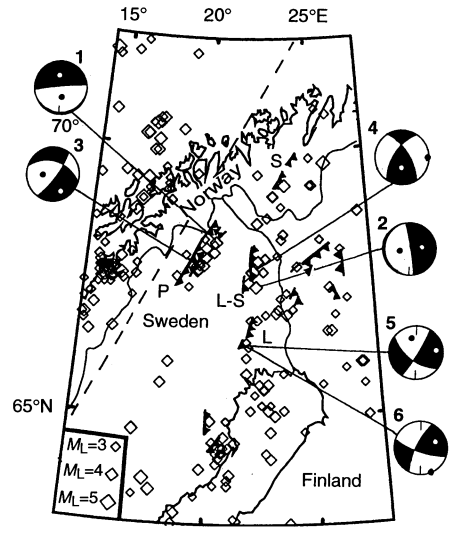

Fig. 1. Earthquake epicenters [diamonds, all with local magnitude M_L(UPP) ≥ 2.7] and focal mechanisms (*10*) (shown as lower hemisphere projections) for some earthquakes in the area and the two events at the Lansjärv fault modeled in this report. L, Lansjärv fault; P, Pärvie fault; L-S, Lainio-Suijavaara fault; and S, Stuoragurra fault. Only earthquakes east of the dotted line were considered in the analysis.

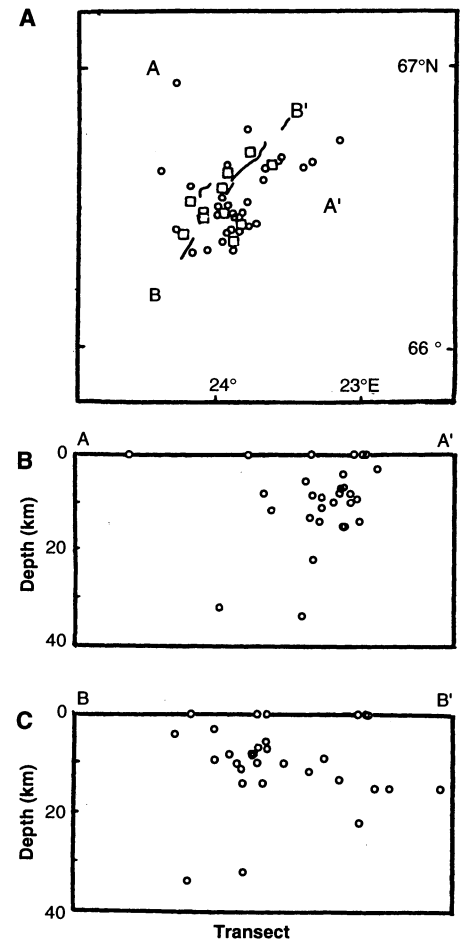

Fig. 2. (**A**) Epicenters of microearthquakes (open circles), $M_L \leq 2.4$, near the Lansjärv fault. Solid line is the fault trace. (**B**) Depth profile for section A–A′. (**C**) Depth profile for section B–B′.

Seismological Department, Uppsala University, Box 2101, S-750 02 Uppsala, Sweden.

*Present address: Department of Earth and Planetary Sciences, Harvard University, 20 Oxford Street, Cambridge 02138, MA, USA.

by large intraplate earthquakes. Concentrations of seismicity that appear to extend beyond the PGFs (Fig. 1) may be attributed to PGFs that did not rupture to the surface or to unrecognized PGFs.

I derived two focal mechanisms (*14*) for events 5 and 6 (Figs. 1 and 3), located at depths of 14 and 34 km, using wave form modeling (*7*). These events, along with event 4 (Fig. 1) at the Lainio-Suijavaara fault, were the only events with relatively near-field recordings, and thus have the best constrained focal mechanisms. Their focal planes coincide with the strike of the fault surface traces. The different faulting styles, as seen in events 1 to 6 (Fig. 1), probably reflect the different stress regime acting today versus the thrust regime active at the time of paleoearthquake occurrence. Focal mechanisms determined from earthquakes near the Stuoragurra fault (*15*) are similar to the focal mechanisms I determined.

The antithetic faults observed at the PGFs may indicate that the dip of the PGFs is shallower at depth (*16, 17*) than observed at the surface (*1, 3*). Even though the modern seismicity is systematically located east of the scarps (Figs. 1 and 2), conforming with the postulated easterly dip (*3*), the poorly resolved focal depths of the regional locations (*10*) do not show how the fault geometry changes at depth. Even from the well-constrained Lansjärv microseismicity the fault dip is not clear, but the two focal mechanisms from the Lansjärv fault, located in the shallow and deep crusts (*14*), do not indicate any change of dip with depth.

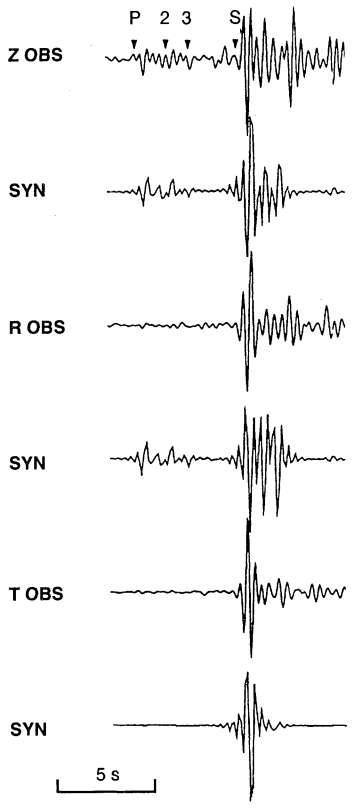

Fig. 3. Observed (OBS) and modeled synthetic (SYN) seismograms for station KAN, for an event of 18 July 1987, $M_L = 2.4$ (*14*). The synthetics are modeled (*6*) at a source depth of 34 km. Z, vertical component; R, radial component, and T, transverse component; P, P wave; S, S wave; 2, downgoing S reflected as upgoing P at the Moho; 3, S wave converted to P wave at Conrad midcrustal interface.

The maximum depth of crustal earthquakes constrains the thickness of the seismogenic zone and the fault width of the PGFs (*18*). Even though most of the focal depths of northern Fennoscandian earthquakes are not well resolved, with the aid of wave form modeling and dense temporary station networks, I determined precise focal depths for 31 Lansjärv microearthquakes (*12*) and a few earthquakes from other PGFs (*7, 8*). The deepest earthquakes associated with PGFs, from the Lansjärv fault and the Lainio-Suijavaar fault, have focal depths of 34 and 37 km, respectively. These depths agree with those of other Baltic Shield earthquakes (*7, 19, 20*) and can be explained (*21*) by the lower crust being brittle because of its relatively low temperature, 400° to 500°C, at the Moho (*22*). Thus, the seismogenic zone extends down to a depth of about 40 km. It may be that the ductile layer in the lower crust is thin or absent in the Baltic Shield. Because faults with lengths larger than the thickness of the seismogenic crust (*18*) extend throughout it, the PGFs probably ruptured down to or close to the Moho. The Moho lies at a depth of 40 to 48 km (*23*) in the east, close to Lansjärv, and on average is more shallow in the western part of the area.

By applying the constant stress drop scaling law for large earthquakes versus fault width, one can write the stress drop as $\Delta\sigma = C\mu D/W$ where C is a constant ranging from about 0.6 to 2 (*24*), μ is the shear modulus, D is the average displacement, and W is the fault width. From the thickness of the seismogenic zone and range of plausible fault dips, the width can be estimated (*25*). Assuming that the fault formed in a single event and using $W = 45 \pm 15$ km, $D = 8 \pm 2$ m (*6*), and $C = 0.65$ for an infinitely long dip-slip fault, I get a stress drop of about 5 MPa ± 2 MPa for the Pärvie fault. For the other PGFs, I obtain estimates of the stress drops of the same order. This is consistent with the stress drops of 3 to 10 MPa estimated for other large earthquakes (*26*). The derived stress drop also explains the large offsets (5 to 15 m) of the PGFs and allows for the rupture process to stay within the crust. Lower stress drops allow several earthquakes to have occurred on the same fault (*17*), but because the PGFs' stress drops fall within the range of other large earthquakes, the one earthquake per fault is the most likely alternative, at least for the faults with average displacements of 10 m and less. This notion also conforms with Quaternary data (*3*), which do not show indications of repeated ruptures, albeit it is not possible to resolve several events within a few years of each other. I derived the size of the cumulative magnitude of the paleoearthquakes by using the same parameters as in the stress-drop calculation (*25*). The calculated moment magnitude for the Pärvie fault was $M_W = 8.2 \pm 0.2$ and for the Lansjärv fault $M_W = 7.8 \pm 0.2$. If the seismogenic zone was 10 km thinner, the magnitudes would be .1 units smaller.

Explanations for the occurrence of PGFs include bending of the crust that causes stress at the edge of the receding ice sheet (*27*) or storage of stress during the time of glaciation (*17, 28*). However, all the faults (Fig. 1) are thrust faults (*3*) and except for the easternmost faults in Finland, the eastern block is elevated with respect to the western block. Thus, I interpret the earthquakes as signs of progressive rapid rise of the land from the center of postglacial rebound, east of the Lansjärv fault, to the outer edges as the ice sheet receded from the center toward the west and finally disappeared. At the start of the last deglaciation, more than 9000 years ago, a nearly isostatic equilibrium was reached due to the depression of the lithosphere by the ice. After a quick removal of the ice sheet a nonisostatic condition caused compressional stresses within the crust, which triggered the earthquakes. Thus, while the addition of ice sheets have been proposed to suppress earthquake occurrence, as in the cases of Greenland and Antarctica (*28*), their removal may cause earthquakes.

REFERENCES AND NOTES

1. R. Kujansuu, *Geol. Surv. Finland Bull.* **256**, 1 (1964); J. Lundqvist and R. Lagerbäck, *Geol. Fören. Stockholm Förh.* **98**, 45 (1976); O. Olesen, *Nor. Geol. Tidsskr.* **8**, 107 (1988).
2. R. Sabadini, K. Lambeck, E. Boschi, Eds., *Glacial Isostasy, Sea-Level and Mantle Rheology* (Kluwer, Dordrecht, Netherlands, 1991).
3. R. Lagerbäck, *Geol. Fören. Stockholm Förh.* **112**, 333 (1990); R. Lagerbäck, *ibid.* **100**, 263 (1979).
4. P. A. Pirazzoli, in (*2*), pp. 259–269.
5. A. C. Johnston, *Geophys. J. Int.* **126**, 314 (1996).
6. L. R. Sykes, *Rev. Geophys. Space Phys.* **16**, 621 (1978); J. W. Dewey, D. P. Hill, W. L. Ellsworth, E. R. Engdahl, *Geol. Soc. Am. Mem.* **172**, 541 (1989).
7. R. Arvidsson and O. Kulhanek, *Geophys. J. Int.* **116**, 377 (1994).
8. W.-Y. Kim, E. Skordas, Y.-P. Zhou, O. Kulhanek, *Swedish Nuclear Fuel Waste Manage. Tech. Rep. 88-23* (1988).
9. T. Ahjos and M. Uski, *Tectonophysics* **207**, 1 (1992).
10. The area covered by earthquakes related to PGFs

was defined by the length times the width. Total length covered by the PGFs is ~500 km. Width, the distance from the fault, 10 km on the footwall side and 50 km on the hanging wall side, was based on mislocation uncertainty of 10 km [R. Arvidsson and R. Wahlström, *Swedish Nuclear Fuel Waste Manage. Tech. Rep. 93-13* (1993)] and surface projection of a 45° dipping fault in a 40-km-deep crust. The area covered by postglacial earthquakes, about 6% of the area east of the dotted line in Fig. 1, contains 48 out of 99 earthquakes, of the investigated area. The statistical probability of this occurrence, estimated as a Poisson process, is almost zero.
11. R. Wahlström, S.-O. Linder, C. Holmquist, H.-E. Mårtensson, *Swedish Nuclear Fuel Waste Manage. Tech. Rep. 89-01* (1989).
12. I located the events by a version of the Hypocenter program [B. R. E. Lienert, *Inst. Solid Earth Physics, Univ. Bergen Tech. Rep.* (1991)], which allows use of S and P arrival times, S-P times (when station clock time was not exact due to poor radio receiving conditions), and azimuths. The azimuths were determined by a maximum likelihood approach [R. G. Roberts and A. Christoffersson, *Geophys. J. Int.* **103**, 55 (1990)]. The exactness of the locations was tested by determining locations from test explosions. The errors ranged from 0.7 to 6 km in the worst case (only three phases and one azimuth). On this basis and the number of recorded phases (out of 31 events, 25 had 5 to 12 phases and the rest 3 to 4 phases, and azimuths), I estimated the typical error to less than 1 km.
13. C. H. Scholz, *The Mechanics of Earthquakes and Faulting* (Cambridge Univ. Press, Cambridge, 1990).
14. The two modeled earthquakes are event 5, on 27 May 1987 (M_L = 2.0, h = 14 km) at 66.64°N and 22.37°E, and event 6 on 18 July 1987 (M_L = 2.4, h = 34 km) at 66.42°N and 21.71°E recorded by mobile networks (*12*). The two focal mechanisms are, for event 5, strike = 30°, dip = 80°, rake = −34°, and for event 6, strike = 205°, dip = 70°, rake = 20°.
15. C. Lindholm, H. Bungum, M. Villagran, E. Hicks, *Proceedings Workshop on Rock Stresses in the North Sea, Trondheim, Norway, 13 to 14 February 1995*, pp. 77–91.
16. C. Talbot, *Swedish Nuclear Fuel Waste Manage. Tech. Rep. 86-20* (1986); H. Henkel, *ibid. Tech. Rep. 88-07* (1988).
17. R. Muir Wood, *ibid. Tech. Rep. 93-13* (1993).
18. S. Das and C. H. Scholz, *Nature* **305**, 621 (1983).
19. W.-Y. Kim, O. Kulhanek, T. van Eck, R. Wahlström, *Rep. 1-85*, Seismological Department, Uppsala University (1985).
20. H. Bungum, A. Alsaker, L. B. Kvamme, R. A. Hansen, *J. Geophys. Res.* **96**, 2249 (1991).
21. W.-P. Chen, *Seismol. Res. Lett.* **59**, 263 (1988); R. Arvidsson, thesis, Uppsala University, Uppsala, Sweden (1991).
22. N. Balling, *Tectonophysics* **244**, 13 (1995).
23. U. Luosto, *ibid.* **189**, 19 (1991).
24. I. P. Parsons, J. F. Hall, G. A. Lyzenga, *Bull. Seismol. Soc. Am.* **78**, 931 (1988).
25. Estimated fault dimensions [L and D determined from data in (*1, 3, 4*)]; Pärvie fault, L = 160 ± 10 km; W = 45 ± 15 km, if the dip varies between 90° and 40° and the seismogenic zone is between 30 and 40 km; displacement is based on averaging of surface measurements, D = 8 ± 2 m; Lansjärv PGF, L = 50 ± 5 km, W = 40 ± 10 km, D = 7 ± 2 m.
26. H. Kanamori and D. L. Anderson, *Bull. Seismol. Soc. Am.* **65**, 1073 (1975).
27. S. Stein *et al.*, in *Earthquakes at North Atlantic Passive Margins: Neotectonics and Postglacial Rebound*, S. Gregersen and P. W. Basham, Eds. (Kluwer, Dordrecht, Netherlands, (1989), pp. 231–259.
28. A. C. Johnston, in *ibid.*, pp. 581–591.
29. I thank R. Roberts and A. Christoffersson for supplying the program for azimuth calculations and G. Ekström, O. Kulhanek, M. Nettles, and two anonymous reviewers for comments. This research was partially supported by the Swedish Natural Research Science Council through projects G-GU 3164-309,312 and the Swedish Foundation for International Cooperation in Research and Higher Education.

21 May 1996; accepted 19 September 1996

Climatic and Hydrologic Oscillations in the Owens Lake Basin and Adjacent Sierra Nevada, California

Larry V. Benson, James W. Burdett, Michaele Kashgarian, Steve P. Lund, Fred M. Phillips, Robert O. Rye

Oxygen isotope and total inorganic carbon values of cored sediments from the Owens Lake basin, California, indicate that Owens Lake overflowed most of the time between 52,500 and 12,500 carbon-14 (^{14}C) years before present (B.P.). Owens Lake desiccated during or after Heinrich event H1 and was hydrologically closed during Heinrich event H2. The magnetic susceptibility and organic carbon content of cored sediments indicate that about 19 Sierra Nevada glaciations occurred between 52,500 and 23,500 ^{14}C years B.P. Most of the glacial advances were accompanied by decreases in the amount of discharge reaching Owens Lake. Comparison of the timing of glaciation with the lithic record of North Atlantic core V23-81 indicates that the number of mountain glacial cycles and the number of North Atlantic lithic events were about equal between 39,000 and 23,500 ^{14}C years B.P.

Evidence of rapid oscillations in air and sea surface temperatures during the last glacial period have been recognized in ice cores from Greenland (*1*) and sediment cores from the North Atlantic (*2*, *3*). Layers of lithic fragments rich in carbonate debris (Heinrich layers) have been found in sediment cores from the temperate North Atlantic and appear to be linked to the dynamics of the Laurentide Ice Sheet and other Northern Hemisphere ice sheets by the discharge of icebergs into the North Atlantic (*3*–*5*). The last four Heinrich events occurred at the end of progressive decreases in sea surface and air temperatures (Dansgaard-Oeschger cycles) and were followed by rapid warmings.

Several authors have attempted to link proxy records of climate change from other areas of the world to Dansgaard-Oeschger cycles and Heinrich events (*6*). In particular, it has been suggested that alpine glaciers in the Rocky Mountains advanced to their terminal areas up to several thousand years before a Heinrich event and retreated soon thereafter (*7*). However, limitations in chronology and sampling resolution have made it difficult to demonstrate that North Atlantic climatic oscillations were synchronous with climatic and hydrologic oscillations in other regions. Here we present continuous, well-dated, high-resolution proxy records of climate change in the Owens Lake basin and compare them with the North Atlantic lithic record documented in core V23-81 (*8*).

Owens Lake is located in the Great Basin of the western United States between the central Sierra Nevada and Inyo-White mountain ranges (Fig. 1). Cool-season orographic precipitation in the Sierra Nevada, mostly from North Pacific sources, supplies >99% of the runoff reaching Owens basin (*9*).

Sediment cores OL90-1 (length, 32.75 m) and OL90-2 (28.20 m) were obtained from the Owens Lake basin in 1990 (Fig. 1) (*10*). Age control for OL90-2 was based on 26 accelerator mass spectrometry (AMS) ^{14}C determinations made on the total organic carbon (TOC) fraction of the cored sediment (Fig. 2) (*11*). Age control for OL90-1 was obtained by matching 30 magnetic susceptibility (χ) features common to both cores. The OL90-2 ^{14}C age–depth polynomial was then applied to OL90-1. A continuous set of sediment samples, 5 to 6 cm in length, was taken from the two cores. Total carbon (TC), total inorganic carbon (TIC), and $\delta^{18}O$ values were determined on each sample (*12*).

To determine if abrupt changes in climate affected the hydrologic balance of the Owens Lake basin, we examined the $\delta^{18}O$ and TIC records (Fig. 3). The $\delta^{18}O$ value (*13*) of a lake represents a balance between amounts and $\delta^{18}O$ values of water input to and lost from a lake. When Owens Lake

L. V. Benson, U.S. Geological Survey, 3215 Marine Street, Boulder, CO 80303, USA.
J. W. Burdett and R. O. Rye, U.S. Geological Survey, MS 963, Denver Federal Center, Lakewood, CO 80225, USA.
M. Kashgarian, Lawrence Livermore National Laboratory, Post Office Box 808, L-397, Livermore, CA 94550, USA.
S. P. Lund, Department of Earth Sciences, University of Southern California, Los Angeles, CA 90089, USA.
F. M. Phillips, Department of Earth and Environmental Science, New Mexico Institute of Mining and Technology, Socorro, NM 87801, USA.